



Quantification of myocardial perfusion reserve by CZT-SPECT: A head to head comparison with ^{82}Rb PET imaging

Wanda Acampa, MD, PhD,^{a,b} Emilia Zampella, MD, PhD,^a Roberta Assante, MD, PhD,^a Andrea Genova, MD,^a Giovanni De Simini, MD,^a Teresa Mannarino, MD,^a Adriana D'Antonio, MD,^a Valeria Gaudieri, MD, PhD,^a Carmela Nappi, MD, PhD,^a Pietro Buongiorno, MS,^a Ciro Gabriele Mainolfi, MD,^a Mario Petretta, MD, FAHA,^c and Alberto Cuocolo, MD^a

^a Department of Advanced Biomedical Sciences, University Federico II, Naples, Italy

^b Institute of Biostructure and Bioimaging, National Council of Research, Naples, Italy

^c Department of Translational Medical Sciences, University Federico II, Naples, Italy

Received Dec 23, 2019; accepted Mar 28, 2020

doi:10.1007/s12350-020-02129-w

Background. We measured myocardial blood flow (MBF) and perfusion reserve (MPR) by dynamic CZT-SPECT and ^{82}Rb -PET in patients with suspected or known coronary artery disease (CAD) and compared the accuracy of the two methods in predicting obstructive CAD.

Methods. Twenty-five patients with available coronary angiography data underwent $^{99\text{m}}\text{Tc}$ -sestamibi CZT-SPECT and ^{82}Rb -PET cardiac imaging. Stress and rest MBF and MPR were calculated by both methods and compared. Diagnostic accuracies of CZT-SPECT and PET were also assessed using a receiver-operator-characteristic curve.

Results. CZT-SPECT yielded similar baseline MBF, but higher hyperemic MBF and MPR values compared to PET. There was a modest correlation between the two methods for MPR ($r = 0.56$, $P < .01$). MPR by CZT-SPECT showed a good ability in identify a reduced MPR by PET, with an area under the curve of 0.85. A MPR cut-off of 2.5 was identified by CZT-SPECT for detection of abnormal MPR by PET, with a sensitivity, specificity and accuracy of 86%, 73% and 80%. The area under the curve for the identification of obstructive CAD by regional MPR were 0.83 for CZT-SPECT and 0.84 for PET ($P = .90$). At CZT-SPECT, a regional MPR of 2.1 provided the best trade-off between sensitivity and specificity for identifying obstructive CAD. Diagnostic accuracy of CZT-SPECT and PET using respective cut-off values was comparable ($P = .62$).

Conclusion. Hyperemic MBF and MPR values obtained by CZT-SPECT are higher than those measured by ^{82}Rb -PET imaging, with a moderate correlation between the two methods. CZT-SPECT shows good diagnostic accuracy for the identification of obstructive CAD. These findings may encourage the use of this new technique to a better risk stratification and patient management. (J Nucl Cardiol 2021;28:2827–39.)

Electronic supplementary material The online version of this article (<https://doi.org/10.1007/s12350-020-02129-w>) contains supplementary material, which is available to authorized users.

The authors of this article have provided a PowerPoint file, available for download at SpringerLink, which summarises the contents of the paper and is free for re-use at meetings and presentations. Search for the article DOI on SpringerLink.com.

The authors have also provided an audio summary of the article, which is available to download as ESM, or to listen to via the JNC/ASNC Podcast.

Reprint requests: Ciro Gabriele Mainolfi, MD, Department of Advanced Biomedical Sciences, University Federico II, Via Pansini 5, 80131 Naples, Italy; c.mainolfi@libero.it
1071-3581/\$34.00

Copyright © 2020 American Society of Nuclear Cardiology.

Key Words: CAD • SPECT • PET • Myocardial blood flow • Diagnostic and prognostic application**Abbreviations**

MPR	Myocardial perfusion reserve
MBF	Myocardial blood flow
CAD	Coronary artery disease
PET	Positron emission tomography
CT	Computed tomography
CZT	Cadmium-zinc-telluride
SPECT	Single photon emission computed tomography
LAD	Left anterior descending
LCx	Left circumflex
RCA	Right coronary artery

See related editorial, pp. 2840–2844**INTRODUCTION**

Noninvasive evaluation of myocardial perfusion reserve (MPR), as result of the ratio of absolute hyperemic to rest myocardial blood flow (MBF), represents a valid tool to increase the diagnostic and prognostic value of myocardial perfusion imaging.¹ In particular, absolute quantification of MPR is useful for the better definition of coronary artery disease (CAD) involvement, such as the different perfusion and functional patterns, including coronary microvascular dysfunction or the diagnosis of multivessel disease.^{2,3} Positron emission computed tomography (PET)/computed tomography (CT) is a well-validated noninvasive method for the quantification of myocardial perfusion imaging studies, demonstrating an incremental diagnostic and prognostic power of MPR over relative perfusion imaging findings in patients with suspected or known CAD.^{4,5} The introduction of novel dedicated cadmium-zinc-telluride (CZT) single-photon emission computed tomography (SPECT) systems allows dynamic acquisition by list mode with quantification of MBF and MPR in addition to standard perfusion and functional parameters.⁶ Prior studies demonstrated that impaired MPR obtained by CZT-SPECT correlates with the presence and severity of CAD.^{7–10} The use of CZT-SPECT systems for the measurement of MPR is very attractive considering that in one examination is possible to obtain perfusion and functional parameters with comparable results to PET imaging. Recently, MBF and MPR measurements from dynamic CZT-SPECT were compared with both ¹⁵O-water and ¹³N-ammonia PET demonstrating a good correlation.^{11,12} For clinic applications, cardiac PET imaging with ⁸²Rb is more extensively used considering that the tracer is generator-produced and it does not require a cyclotron in site,

containing the costs with a higher rate of studies performed.¹³ The aim of the present study was to measure MBF and MPR by dynamic CZT-SPECT and ⁸²Rb-PET/CT in a cohort of patients with suspected or known CAD and available coronary angiography data and to compare the accuracy of the two methods in predicting obstructive CAD.

MATERIALS AND METHODS**Study Population**

The study population included 231 patients with suspected or known CAD referred to stress/rest SPECT myocardial perfusion imaging for clinical evaluation. Fifty-eight of these patients were submitted to cardiac PET within two weeks (average 7 ± 5 days) for MBF quantification, as needed adjunct to the image findings, to better identify or exclude multivessel CAD, for improved risk stratification, and when assessment of microcirculatory function was needed for clinical decision making.¹⁴ No revascularization procedure or medical therapy optimization was performed between CZT-SPECT and PET studies. Of these latter patients, 25 with positive perfusion imaging or reduced MPR were referred for invasive coronary angiography within 90 days after perfusion imaging (average 49 ± 23 days) to consider revascularization.

The decision to send patients to angiography was made by the referring physicians. Patient clinical history was collected and cardiac risk factors were assessed before imaging. Atypical angina was defined as the presence of two criteria including substernal chest pain or discomfort, with characteristic quality and duration, provoked by exertion or emotional stress and relieved by rest and/or nitrates according to the Diamond Classification.¹⁵ Hypertension was defined as a blood pressure $\geq 140/90$ mmHg or the use of anti-hypertensive medication. Hypercholesterolemia was defined as total cholesterol level > 6.2 mmol/L or treatment with cholesterol lowering medication. Patients were classified as having diabetes if they were receiving treatment with oral hypoglycemic drugs or insulin. A positive family history of CAD was defined by the presence of disease in first-degree relatives younger than 55 years in men or 65 years in women. Patients with previous myocardial infarction ($n = 10$) and/or revascularization ($n = 13$) were considered as having known CAD. This study complies with the declaration of Helsinki. The review committee of our institution approved this study and all patients gave informed consent (“Comitato Etico, Università Federico II”, protocol number 110/17).

CZT-SPECT Imaging

All patients performed a 1-day rest-stress protocol (Figure 1). Patients were instructed not to consume products containing caffeine for 24 hours before the test. Myocardial

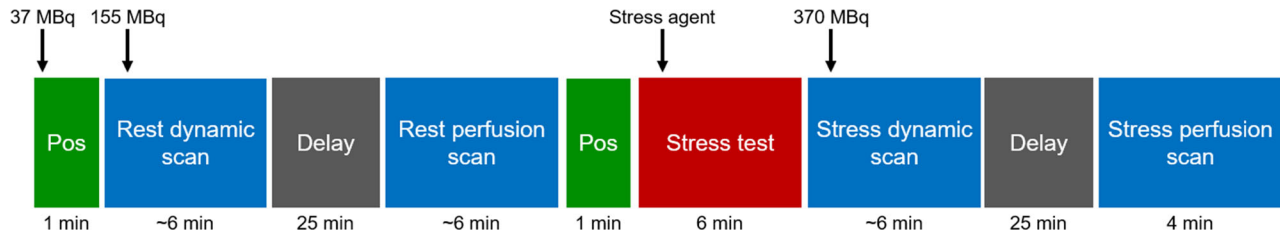


Figure 1. Dynamic CZT-SPECT imaging protocol. An initial dose of approximately 37 MBq is administered in order to position (Pos) the patient’s heart within the field of view using a 60-seconds pre-scan acquisition. A dose of 155 MBq is then injected to the patient as a bolus with a dynamic list-mode images acquisition. After a delay of 25 minutes a rest gated perfusion scan is acquired. After controlling the correct position of the heart a dipyridamole infusion was started. A second bolus of tracers was injected for dynamic stress by a list-mode acquisition of 6 minutes with a subsequent stress gated acquisition of 4 minutes.

perfusion imaging was performed in upright position using a dedicated cardiac CZT camera (DSPECT, Spectrum Dynamics, Caesarea, Israel). A dose of 37 MBq of ^{99m}Tc -sestamibi was administered for a 60-seconds pre-scan acquisition to check patient position, to identify the location of the heart and to set the angle limits of scanning for each detector (region of interest—centric scanning). For rest dynamic images, an intravenous bolus administration of 155 MBq of ^{99m}Tc -sestamibi at rate of 1 to 2 $\text{cm}^3\cdot\text{s}^{-1}$ using an automatic injector system (Empower CTA, Bracco Imaging Italia, Milano, Italy) and flushed by 30 mL of saline to ensure consistent delivery of a tight bolus. From the injection time a list-mode acquisition of 6 minutes started. Pharmacologic stress test using dipyridamole was started. Dipyridamole was infused at dose of 0.56 $\text{mg}\cdot\text{kg}^{-1}$ intravenously over a 4-minute period (140 $\text{mcg}\cdot\text{kg}^{-1}\cdot\text{min}^{-1}$). All along the infusion, monitoring of heart rate and rhythm, blood pressure, and electrocardiography (ECG) were performed. Four minutes after completion of dipyridamole infusion, a second bolus of 370 MBq of ^{99m}Tc -sestamibi was injected for dynamic stress acquisition followed by a list-mode acquisition of 6 minutes. At the end of the dynamic stress acquisition, a dose of 100 mg of aminophylline was administered intravenously in the event of chest pain or other symptoms, or after significant ST depression. List-mode data were rebinned into 32 frames consisting of 21×3 , 1×9 , 1×15 , 1×21 , 1×27 and 7×30 second frames.¹¹ An ordered subset expectation maximization algorithm was used for image reconstruction with 4 iterations and 32 subsets (smoothing factor 0.125 IIF). No post filter or temporal filters in between frames were applied.

PET/CT Imaging

As a routine preparation for ^{82}Rb cardiac PET/CT, patients were asked to discontinue taking nitrates for 6 hour, calcium channel blockers and caffeine-containing beverages for 24 h, and beta-blockers for 48 hour before their appointment. Scans were acquired using a Ingenuity TF 64 scanner (Philips). Rest and stress cardiac PET/CT images were acquired as follows: scout CT was performed to check patient position and low-dose CT [0.4 mSv; 120 kVp; effective tube

current, 26 mA (11-mAs quality reference); 3.3 second] was performed for attenuation correction, during normal breathing before and after PET acquisitions. For both rest and stress imaging a mean dose of 740 MBq of ^{82}Rb was injected by using an automated infusion system (Cardiogen-82®) with a 6-minute list-mode PET acquisition. The infusion system ensures accurate dosing with minimal operator interface and minimizes the radiation exposure. The infusion parameters were set as follows: elution volume 60 mL; patient volume 30 mL. After rubidium elution, a saline flush was performed for the bolus and to wash infusion system. Pharmacologic stress was then induced by administration of dipyridamole over a 4-minute period (140 $\text{mcg}/\text{kg}/\text{min}$). Rest and stress dynamic images were reconstructed into 26-time frames (12×5 , 6×10 , 4×20 , and 4×40 second) using the vendor standard ordered subsets expectation maximization 3D reconstruction (2 iterations, 24 subsets) with 6.5-mm Gaussian post-processing filter. CT-based attenuation, scatter, decay, and random corrections were applied to the reconstructed images. The heart rate, systemic blood pressure, and 12-lead ECG were recorded at baseline and throughout the infusion of dipyridamole.

Imaging Analysis

For both CZT-SPECT and PET/CT imaging, an automated software program (e-soft, 2.5, QGS/QPS, Cedars- Sinai Medical Center, Los Angeles, CA, USA) was used to calculate the scores incorporating both the extent and severity of perfusion defects, using a standardized segmentation of 17 myocardial regions. A summed stress score < 3 was considered normal.

Dynamic CZT-SPECT Imaging

Dynamic CZT-SPECT imaging data were analyzed using commercially available Corridor 4DM software (v2017, INVIA, Ann Arbor, MI, USA), as previously described in detail.¹¹ The correction factor for myocardial density was set to 1, the spillover from the blood pool activity to the myocardium to 0.40, and the spillover from the myocardium to the blood pool activity to 0.0 assuming the spillover is

negligible. Integration limit t_1 denotes the end of the blood pool phase, typically at 1.5 minute, while t_2 and t_3 denote integration limits of the average tissue activity, typically from 1.5 to 2.5 minute. The integration limits were adjusted to the peak of the blood time activity curves. Baseline MBF values were adjusted for the patient-specific rate-pressure product. Global and regional MPR for left anterior descending (LAD), left circumflex (LCx), and right coronary artery (RCA) were defined as the ratio of hyperemic to baseline MBF.

Dynamic PET Imaging

From dynamic PET imaging data, absolute MBF was computed (in milliliters per minute per gram) and quantified using a one-compartment constant distribution volume model from the dynamic rest and stress imaging series with commercially available software (FlowQuant version 2.4, University of Ottawa Heart Institute).¹⁶ Transaxial dynamic images were automatically reoriented to short-axis slices. A spline model of the left ventricular myocardium was fit to the short-axis images averaged from 2 to 6 minute. The myocardial segmentation and the definition of the input function from the left ventricular cavity were performed automatically, with optional user adjustments when needed. Global spillover and regional partial-volume corrections were performed using geometric mixing models.¹⁷ Baseline MBF values were adjusted for the patient-specific rate-pressure product. Global and regional MPR (for LAD, LCx, and RCA) were defined as the ratio of hyperemic to baseline MBF. At PET imaging, reduced MPR was defined as < 2 for global values and < 1.64 for regional measurements.^{4,5}

Coronary Angiography

Coronary angiography was performed using the standard Judkins method. Experienced cardiologists visually interpreted all coronary angiograms. Presence of luminal diameter stenosis $\geq 70\%$ in at least one of the major vascular territories was considered as obstructive CAD.^{18,19}

Statistical Analysis

Continuous variables were expressed as mean \pm standard deviation and categorical data as frequencies or percentage. Comparison of continuous data between groups was performed using the two-sided Student's t test. The differences for paired data were tested using the McNemar test. A P value $< .05$ (two-sided) was considered statistically significant. Correlation between MPR by CZT-SPECT and by PET has been evaluated by Pearson's coefficient. The differences between the two methods were assessed by Bland-Altman analysis.²⁰ Receiver operating characteristic areas under the curve were used to evaluate the diagnostic ability of global and regional MPR by CZT-SPECT for predicting a reduced MPR by PET and identifying obstructive CAD. The maximum value of the Youden index J was used as a criterion for selecting the optimum cut-off point with the best compromise between sensitivity and specificity for different regional MFR cut-off

points.²¹ Statistical analysis was performed with Stata 15.1 software (StataCorp, College Station, Texas USA).

RESULTS

Clinical characteristics of the study population are summarized in Table 1. The baseline and hyperemic hemodynamic parameters are shown in Table 2. As depicted, a significant response to pharmacological stress test was observed for both imaging procedures (all $P < .001$). Myocardial perfusion was normal in 10 patients and abnormal in 15 patients at both CZT-SPECT and PET imaging. In patients with abnormal myocardial perfusion summed stress score (14 ± 15 vs. 15 ± 10 , $P = .89$), summed rest score (6 ± 9 vs. 7 ± 13 , $P = .86$) and summed difference score (8 ± 7 vs. 8 ± 3 , $P = .48$) were not different between the two methods.

COMPARISON OF CZT-SPECT AND PET FINDINGS

Per-patient Analysis

The correlation of hyperemic MBF between CZT-SPECT and PET was 0.44 ($P < .05$) (Figure 2). At Bland-Altman analysis, the mean difference in hyperemic MBF was 0.46 ± 0.88 , and the lower and upper limits of agreement between CZT-SPECT and PET were -1.26 and 2.18 (Figure 2). A moderate albeit significant correlation of global MPR between CZT-SPECT and PET ($r = 0.56$, $P < .01$) was found (Figure 3). At Bland-Altman analysis, the mean difference in MPR was 0.45 ± 0.68 , and the lower and upper limits of agreement

Table 1. Clinical characteristics of 25 patients with suspected or known CAD

Characteristics	Value
Age (years)	61 \pm 13
Male gender, n (%)	19 (76%)
Atypical angina, n (%)	11 (44%)
Body mass index (kg m^{-2})	28 \pm 5
Diabetes, n (%)	10 (40%)
Hypertension, n (%)	20 (80%)
Hypercholesterolemia, n (%)	14 (56%)
Smoking, n (%)	12 (48%)
Family history of CAD, n (%)	14 (56%)
Known CAD, n (%)	13 (52%)

Values are means \pm standard deviation or number (percentage) of patients
CAD, coronary artery disease

Table 2. Hemodynamic response to stress test during CZT-SPECT and PET procedures in 25 patients with suspected or known CAD

	CZT-SPECT	PET	P value
Baseline heart rate (bpm)	65 ± 9	63 ± 8	.13
Hyperemic heart rate (bpm)	79 ± 12*	80 ± 13*	.77
Baseline systolic BP (mm Hg)	126 ± 14	130 ± 16	.19
Hyperemic systolic BP (mm Hg)	108 ± 10*	115 ± 14*	.08
Baseline diastolic BP (mm Hg)	76 ± 6	80 ± 7	.06
Hyperemic diastolic BP (mm Hg)	70 ± 5*	72 ± 8*	.17
Baseline RPP (10 ³ mmHg/min)	8.1 ± 1.6	8.4 ± 1.9	.21
Hyperemic RPP (10 ³ mmHg/min)	8.5 ± 1.7	9.4 ± 2.1	.08

Values are mean ± standard deviation

CAD, coronary artery disease; BP, blood pressure; RPP, rate-pressure product

* $P < .001$ hyperemic vs. baseline

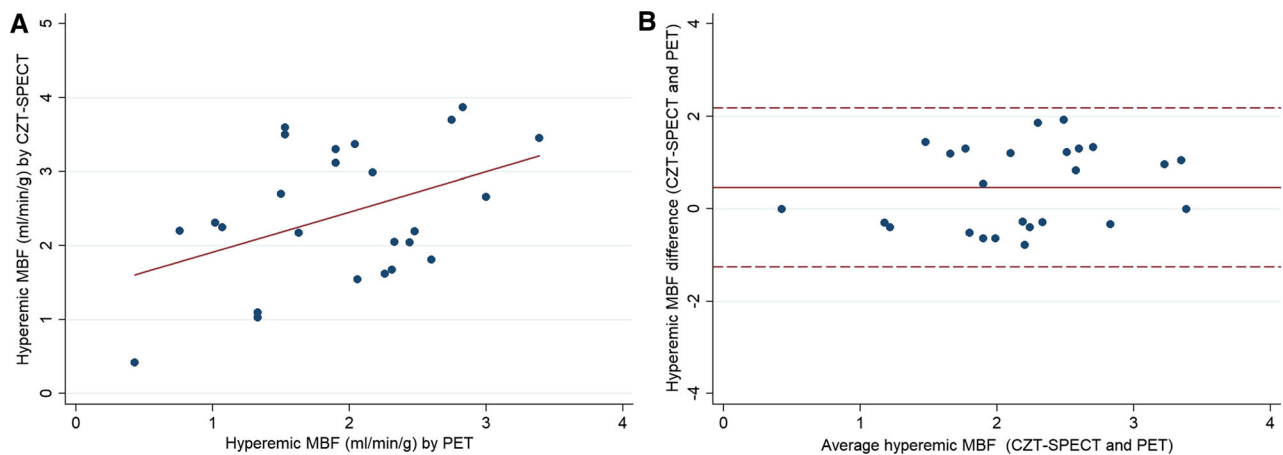


Figure 2. Relationship between hyperemic myocardial blood flow (MBF) by CZT-SPECT and PET (A). Agreement between CZT-SPECT and PET by Bland-Altman analysis for hyperemic MBF measurement. The differences between the two systems are plotted against the means of the two systems. The horizontal red line indicates the mean difference between the two systems and the plotted lines indicate the limits of agreement (B).

between CZT-SPECT and PET were -0.89 and 1.80 (Figure 3). Global baseline and hyperemic MBF and MPR values by CZT-SPECT and PET imaging are shown in Figures 4 and 5. Compared to PET, CZT-SPECT yielded similar baseline MBF values (0.99 ± 0.3 vs. 1.08 ± 0.4 , $P = .29$). Differently, hyperemic MBF (2.40 ± 0.9 vs. 1.94 ± 0.7 , $P < .05$) and MPR (2.44 ± 0.7 vs. 1.99 ± 0.7 , $P < .01$) were significantly higher for CZT-SPECT compared to PET. At receiver operating characteristic curve analysis, global MPR quantification by CZT-SPECT showed a good ability in identify a reduced MPR by PET, with area under the curve of 0.85 (95% confidence interval, CI 0.68 to 1.00). At CZT-SPECT, a MPR cut-off of 2.5 was identified for

detection of abnormal MPR by PET, with a sensitivity, specificity and accuracy of 86% , 73% and 80% .

Per-Vessel Analysis

There was a moderate correlation between CZT-SPECT and PET for MPR values in LAD ($r = 0.52$), LCX ($r = 0.55$) and RCA ($r = 0.52$) territories (all $P < .05$) (Figure 6). At Bland-Altman analysis, the mean difference in MPR was 0.43 ± 0.72 (lower and upper limits of agreement -0.98 and 1.84) in LAD, 0.45 ± 0.68 (lower and upper limits of agreement -0.88 and 1.78) in LCx and 0.47 ± 0.92 (lower and upper limits of agreement -1.33 and 2.27) in RCA territories

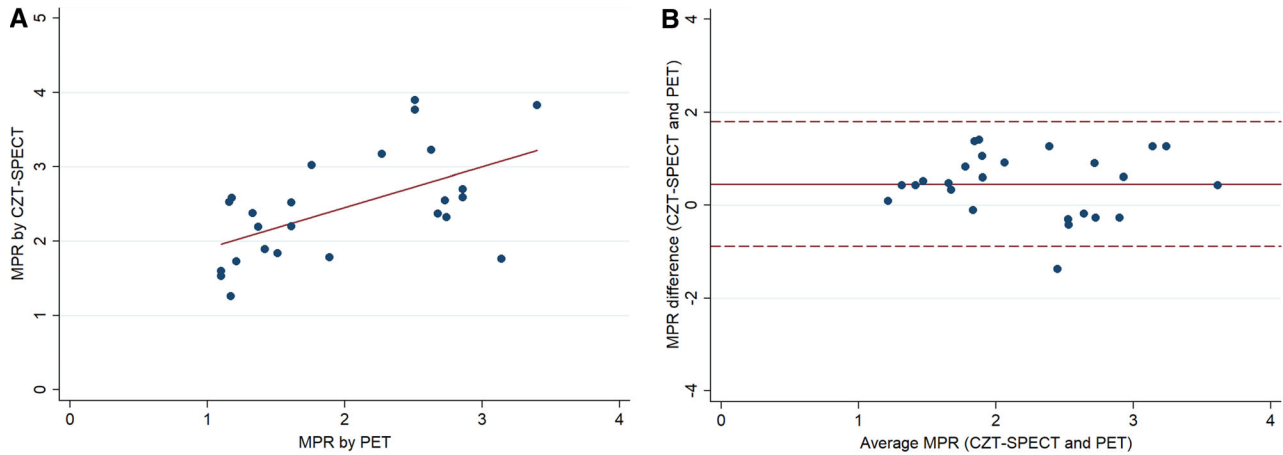


Figure 3. Relationship between myocardial perfusion reserve (MPR) by CZT-SPECT and PET (A). Agreement between CZT-SPECT and PET by Bland-Altman analysis for MPR measurement. The differences between the two systems are plotted against the means of the two systems. The horizontal red line indicates the mean difference between the two systems and the plotted lines indicate the limits of agreement (B).

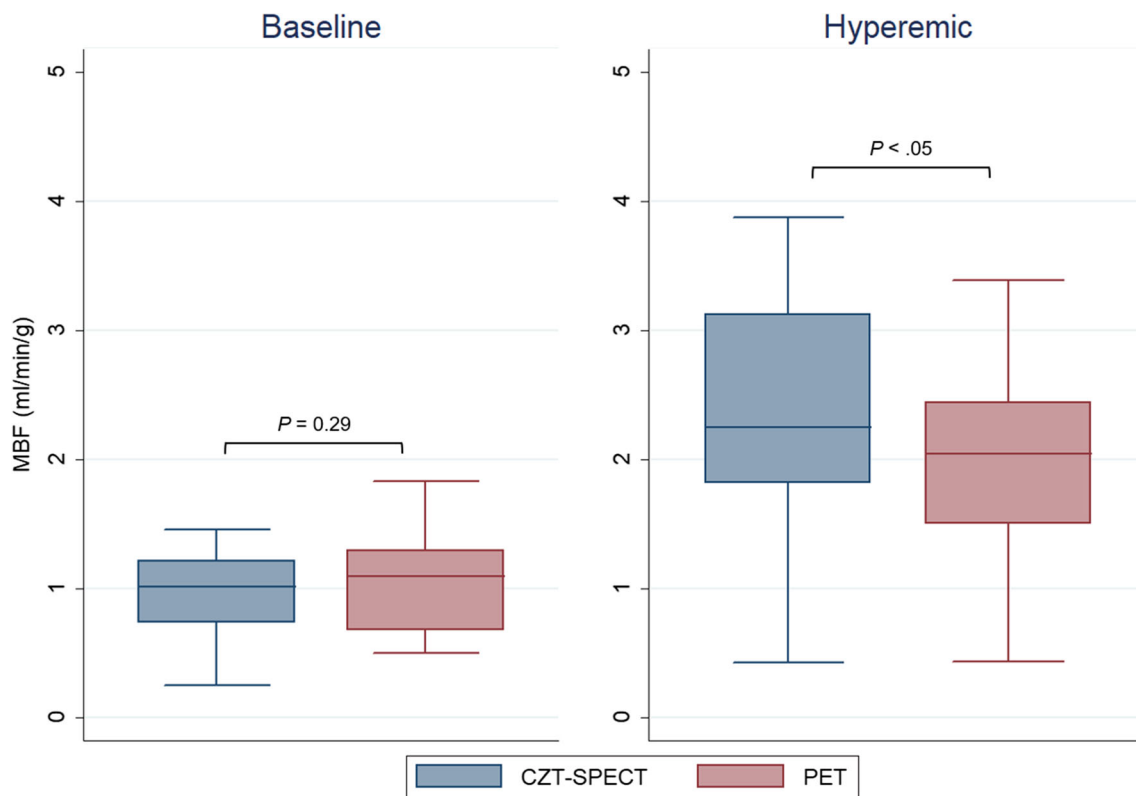


Figure 4. Global baseline and hyperemic myocardial blood flow (MBF) according to CZT-SPECT and PET imaging.

(Figure 6). Regional baseline and hyperemic MBF and MPR values by CZT-SPECT and PET in the main vascular territories are shown in Table 3. In RCA

territory, baseline MBF were significantly lower for CZT-SPECT compared to PET ($P < .01$), with no difference in hyperemic MBF (Figure 7). Differently, in

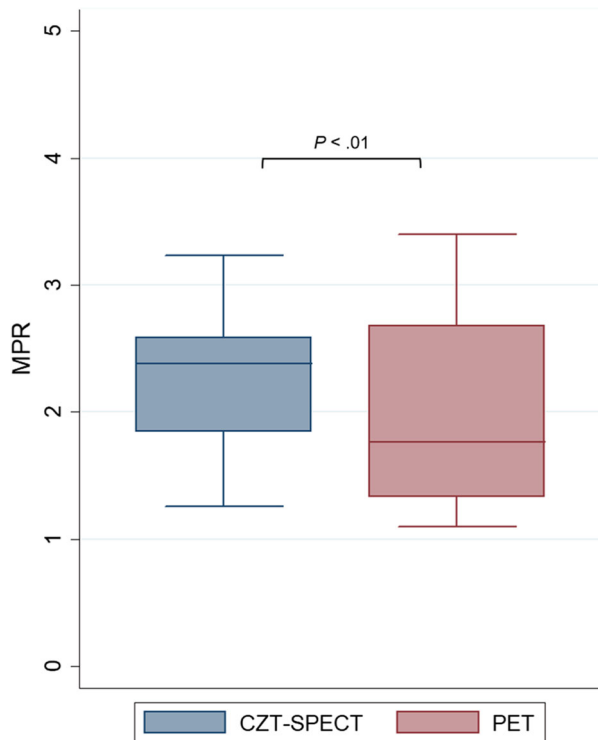


Figure 5. Global myocardial perfusion reserve (MPR) according to CZT-SPECT and PET imaging.

LAD and LCx territories, no differences in baseline MBF were observed, while a higher hyperemic MBF ($P < .01$) was found by CZT-SPECT. Finally, MPR values

were significantly higher for CZT-SPECT compared to PET among all three vascular territories (Figure 8).

Diagnostic Performance in Identify Obstructive CAD

Of the 25 patients enrolled, 7 patients (28%) showed obstructive CAD at coronary angiography. Of these last patients, 2 (29%) had single-vessel disease, 4 (57%) two-vessel disease and 1 (14%) three-vessel disease. Therefore, among the 75 individual vessels analyzed, obstructive CAD was observed in 13 (17%) vessels. During hyperemia, baseline MBF increased significantly in both vessels with and without obstructive CAD (all $P < .01$) (Table 4). Vessels with obstructive CAD compared to those without had lower regional hyperemic MBF and MPR (all $P < .05$) in both modalities. In both vessels with and without obstructive CAD, hyperemic MBF and MPR by CZT-SPECT were significantly higher compared to PET. At receiver operating characteristic curve analysis, the areas under the curve for the identification of obstructive CAD by MPR were 0.83 (95% CI 0.73 to 0.92) for CZT-SPECT and 0.84 (95% CI 0.75 to 0.93) for PET ($P = .90$) (Figure 9). At CZT-SPECT, a regional MPR of 2.1 provided the best trade-off between sensitivity and specificity for identifying obstructive CAD. Diagnostic performance of CZT-SPECT and PET using respective cut-off values to identify obstructive CAD resulted not

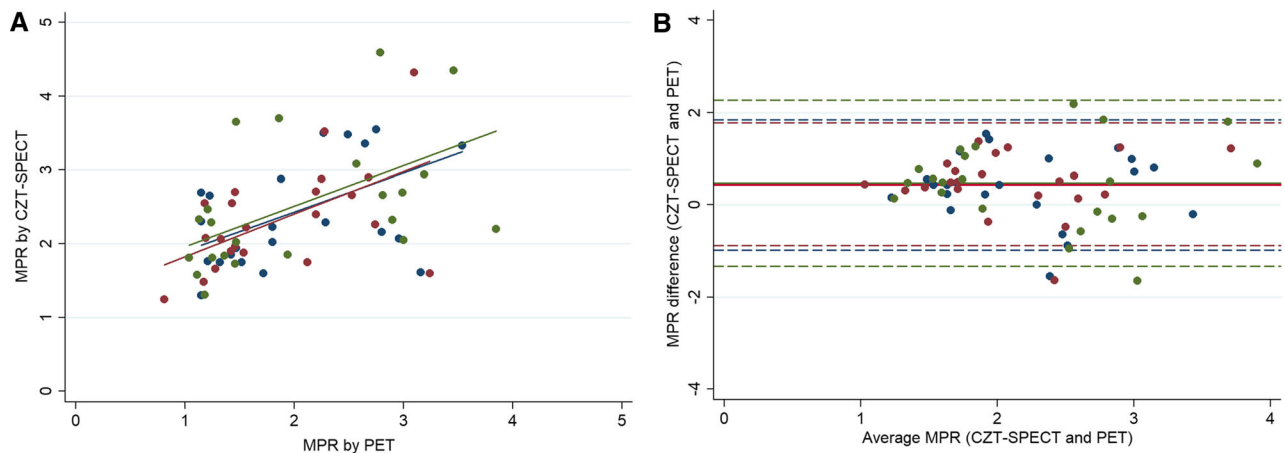


Figure 6. Relationship between myocardial perfusion reserve (MPR) by CZT-SPECT and PET in left anterior descending (LAD) (blue), left circumflex (LCx) (red) and right coronary (RCA) (green) artery territory (A). Agreement between CZT-SPECT and PET by Bland-Altman analysis for MPR measurement in LAD (blue), LCx (red), RCA (green) territory. The differences between the two systems are plotted against the means of the two systems. The horizontal line indicates the mean difference between the two systems and the plotted lines indicate the limits of agreement (B).

Table 3. Regional baseline and hyperemic MBF and MPR by dynamic CZT-SPECT and PET in 25 patients with suspected or known CAD

	Baseline MBF (ml/min/g)			Hyperemic MBF (ml/min/g)			MPR		
	CZT-SPECT	PET	P value	CZT-SPECT	PET	P value	CZT-SPECT	PET	P value
LAD	1.14 ± 0.4	1.07 ± 0.4	.51	2.64 ± 0.9*	1.93 ± 0.7*	< .01	2.43 ± 0.7	2.00 ± 0.7	< .01
LCx	1.10 ± 0.3	1.00 ± 0.4	.31	2.52 ± 0.9*	1.71 ± 0.7*	< .01	2.33 ± 0.6	1.88 ± 0.7	< .01
RCA	0.80 ± 0.3	1.15 ± 0.5	< .01	2.07 ± 0.8*	2.18 ± 1*	.52	2.56 ± 0.9	2.09 ± 0.9	< .05

Values are mean ± standard deviation

MBF, myocardial blood flow; MPR, myocardial perfusion reserve; CAD, coronary artery disease; LAD, left anterior descending artery; LCx, left circumflex artery; RCA, right coronary artery

* $P < .001$ hyperemic vs. baseline

significantly different between the two imaging modalities (Figure 10).

DISCUSSION

The results of this study demonstrated that in patients with suspected or known CAD there is a moderate relationship between MPR values obtained by ^{99m}Tc -sestamibi CZT-SPECT and by ^{82}Rb PET cardiac imaging. Yet, global MPR by CZT-SPECT had a good accuracy in the identification of reduced MPR by PET. The two methods also showed similar results in the identification of obstructive CAD in corresponding coronary arteries.

Recent advances in SPECT technology, related to the introduction of dedicated cardiac cameras with CZT detectors and software-based resolution recovery, helped to overcome most of the limitation of traditional systems.²² It has been demonstrated that quantification of MBF and MPR by list-mode dynamic CZT-SPECT is technically feasible and clinically useful.^{6,7} Ben-Haim et al.⁶ in 95 patients with suspected or known stable CAD, showed that global and regional MPR by CZT-SPECT have a good correlation with total perfusion defect. Moreover, in a subgroup of 16 patients with available angiographic data, global MPR correlated inversely with the extent of obstructive CAD.⁶

Nowadays, PET is still a gold standard for noninvasive assessment of MPR with an excellent diagnostic and prognostic value.^{4,5} Recent data showed a good correlation between CZT-SPECT and PET findings using different tracers and cameras.^{11,12} Nkoulou et al.¹² in 28 patients referred to perfusion imaging with either CZT-SPECT and PET for clinical evaluation of CAD showed an overall good correlation between ^{99m}Tc -tetrofosmin CZT-SPECT and ^{13}N -ammonia PET MBF values ($r = 0.62$, $P < .001$). However, MPR values

by CZT-SPECT were lower compared to those obtained by ^{13}N -ammonia PET, probably due to higher ^{13}N -ammonia extraction fraction at resting conditions over a larger range of MBF. Using a MPR cut-off value of 1.26 calculated by receiver operating characteristic curve analysis, these authors showed an accuracy of 75% by CZT-SPECT in predicting an abnormal PET MFR (i.e., < 2).¹⁰ Agostini et al.¹¹ in 30 patients with stable CAD showed that dynamic CZT-SPECT provides good correlation of MPR values compared to ^{15}O -water PET imaging. The hyperemic and baseline MBF by CZT-SPECT were significantly higher compared to ^{15}O -water PET, with similar MPR values between the two techniques. Moreover, CZT-SPECT data demonstrated high diagnostic value for detecting impaired MPR and abnormal fractional flow reserve in patients with stable CAD.¹¹ Despite ^{15}O -water and ^{13}N -Ammonia are well validate for MBF and MPR quantification, the most commonly used cardiac PET perfusion tracer is ^{82}Rb , which is generator-produced and it does not require a cyclotron in site.¹³ In our study we directly compared dynamic low-dose ^{99m}Tc -sestamibi CZT-SPECT with ^{82}Rb PET for noninvasive quantitative measurement of MBF and MPR. We found a moderate correlation of global and regional MPR values between CZT-SPECT and PET. Also, despite similar global baseline MBF values by CZT-SPECT and PET imaging, we observed higher global hyperemic MBF and MPR by CZT-SPECT compared to PET imaging.

Comparing these findings to previous published data,^{11,12} it should be considered that the different PET perfusion tracers show different physical and biochemical properties.²³ ^{82}Rb has lower extraction (40% to 70%) compared to ^{13}N -ammonia and ^{15}O -water, despite the advantages of higher retention rate and optimal images quality.²⁴ ^{99m}Tc -labeled SPECT tracers show lower extraction fraction that is related to the flow,

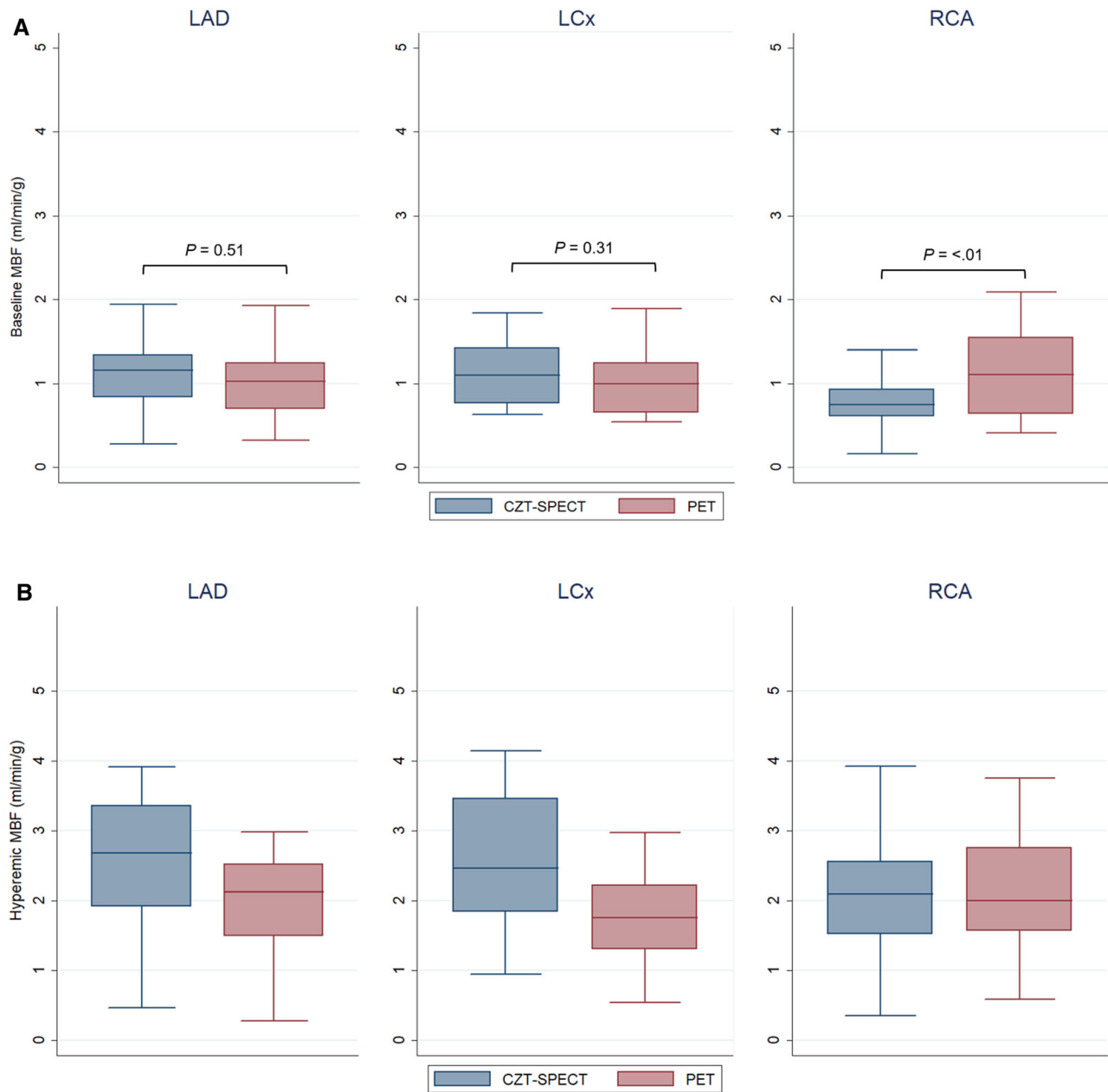


Figure 7. Regional baseline (A) and hyperemic (B) myocardial blood flow (MBF) according to CZT-SPECT and PET imaging in left anterior descending (LAD), left circumflex (LCx) and right coronary (RCA) artery territory.

showing kinetic properties more similar to ^{82}Rb . At regional analysis, we found similar value of baseline MBF in the RCA territory comparing CZT-SPECT to PET despite a higher flow value by CZT-SPECT in the others vascular territories. This result might be explained considering that other factors may have an impact on MBF quantification with the CZT-SPECT.^{25,26} At Bland-Altman analysis we found the limits of agreement wider than those reported in prior

studies.^{11,12,25,26} These differences are probably related to the various methodological approaches used in terms of tracers, camera and correction factors. Wells et al.²⁵ compared MBF and MPR values obtained by CZT-SPECT and PET imaging in 32 patients with known CAD (6 with ^{13}N -ammonia PET and 25 with ^{82}Rb) to assess the incremental value of corrections for body motion, blood binding, and attenuation in MBF quantification. They found that global MBF accuracy was

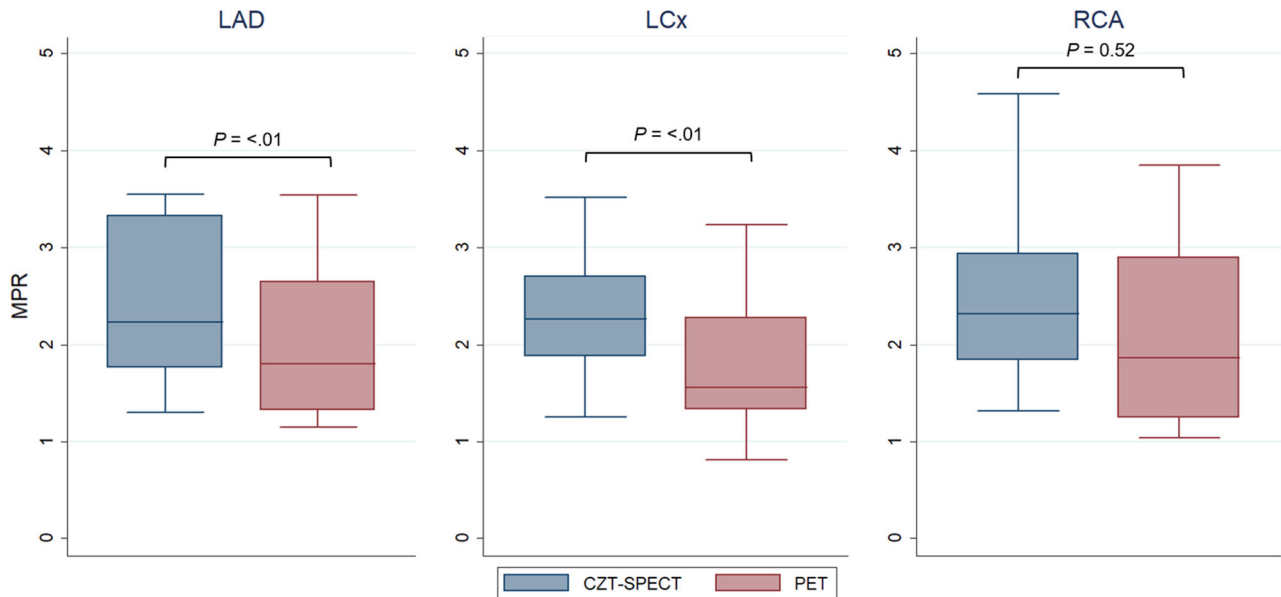


Figure 8. Regional myocardial perfusion reserve (MPR) according to CZT-SPECT and PET imaging in left anterior descending (LAD), left circumflex (LCx) and right coronary (RCA) artery territory.

Table 4. Imaging findings estimates by dynamic CZT-SPECT and PET in vessels with and without obstructive CAD

	CZT-SPECT			PET		
	With CAD (n = 13)	Without CAD (n = 62)	P value	With CAD (n = 13)	Without CAD (n = 62)	P value
Baseline MBF (ml/min/g)	1.02 ± 0.4	1.01 ± 0.4	.94	1.07 ± 0.3	1.07 ± 0.5	.96
Hyperemic MBF (ml/min/g)	1.80 ± 0.7* [§]	2.54 ± 0.9* [§]	< .01	1.31 ± 0.5*	2.07 ± 0.8*	< .01
MPR	1.76 ± 0.3	2.59 ± 0.7	< .001	1.23 ± 0.2	2.15 ± 0.8	< .001

Values are mean ± standard deviation

CAD, coronary artery disease; MBF, myocardial blood flow; MPR, myocardial perfusion reserve

* $P < .001$ hyperemic vs. baseline

[§] $P < .05$ CZT-SPECT vs. PET

improved with motion and blood binding but not with attenuation correction. Giubbini et al.²⁶ comparing CZT-SPECT and ¹³N-ammonia PET results found a significant impact of attenuation correction on MBF measurements. In particular, MBF seems to be slightly overestimated when attenuation correction is not applied. Therefore, there is a need to better elucidate the potential role of methodological differences between CZT-SPECT and PET for quantitative cardiac imaging.

In agreement with previous studies,^{11,12} we identified high sensitivity (86%) and accuracy (80%) by CZT-

SPECT for the detection of impaired PET flow reserve. Despite the differences in tracers kinetic, CZT-SPECT and PET showed similar clinical findings. We analyzed regional perfusion in patients with available coronary angiographic data, to compare the diagnostic capability of CZT-SPECT and PET in identify obstructive CAD. As expected, for both imaging modalities similar baseline MBF values, but lower hyperemic MBF and MPR values, were observed in vessels with CAD as compared to those without. At receiver operating characteristic curve analysis, CZT-SPECT and PET showed similar

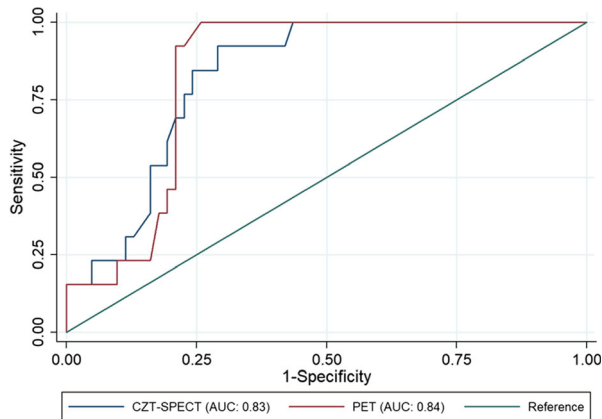


Figure 9. Receiver operating characteristic curves for identifying coronary artery stenosis $\geq 70\%$ for MPR quantification using CZT-SPECT vs. PET imaging.

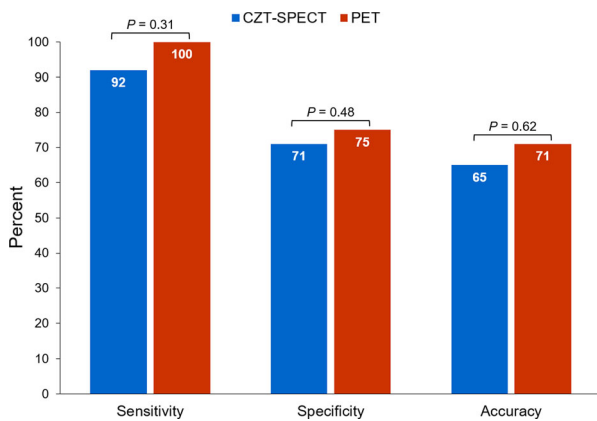


Figure 10. Comparison of diagnostic performance of CZT-SPECT and PET imaging to identify obstructive CAD in 75 vascular territories.

diagnostic performance in identify the presence of obstructive CAD. The ability of MPR obtained by CZT-SPECT in identify obstructive CAD was assessed by previous reports, and different cut-off points have been proposed. The accuracy of dynamic CZT-SPECT in detecting obstructive CAD has been recently investigated.^{7,27} de Souza et al.⁷ found a similar regional cut-off of 2.2 in identifying obstructive lesions. In the present study, a regional cut-off of 2.1 was identified as the best trade-off between sensitivity (91%) and specificity (71%) in identify obstructive CAD with similar sensitivity, specificity and accuracy compared to PET. Acampa et al.²⁷ in a different and larger population identified a regional MPR cut-off point of 2.1 for the identification of obstructive lesions in the corresponding coronary artery and showed some differences in sensitivity (65% vs. 92%, $P = .04$) and specificity (83% vs. 71%, respectively, $P = .07$) compared to the present investigation. The difference in sensitivity could be

explained with the more selective patient population referred to PET imaging in the present study inducing a lower number of false positive results.

In the present study CZT-SPECT imaging has been obtained by using a low-dose protocol. Our data support the important role of CZT systems in reducing the administered dose in an era where dose-saving strategies enable nuclear cardiology to be more cost-effective and improving patient and medical staff protection.

Our results are limited by the small number of patients enrolled, in particular those with severe stenosis, and by PET scanner used. A possible detector saturation effect may have contributed to the measured differences between SPECT and PET flow on our scanner, which has quite limited dynamic range.^{28,29} However, for each patient saturation effect was evaluated visually upon identification of plateau-like peaks occurring at the first-pass of the tracer-bolus from the input functions obtained in the left ventricle. Evaluation of the general image quality of the dynamic frames was also performed. Finally, variability among prior studies and the present investigation should also consider the differences between the methodologies, myocardial radiotracer distribution, reconstruction algorithms, and flow model applied. More studies with larger number of patients are needed.

NEW KNOWLEDGE GAINED

Our study adds new information about the absolute quantification of MBF and MPR by CZT-SPECT. In particular, it indicates that quantitative measurements provided by CZT-SPECT are related to those obtained by ⁸²Rb PET cardiac imaging, with good diagnostic performance in the identification of obstructive CAD.

CONCLUSION

Hyperemic MBF and MPR values obtained by dynamic CZT-SPECT are higher than those obtained by ⁸²Rb PET cardiac imaging, with a moderate correlation between the two methods. CZT-SPECT show good diagnostic accuracy for the identification of obstructive CAD, with sensitivity and specificity values similar to PET. These findings may encourage the use of this new technique to a better risk stratification and patient management.

Disclosures

W Acampa, E Zampella, R Assante, A Genova, G De Simini, T Mannarino, A D'Antonio, V Gaudieri, C Nappi, P Buongiorno, C.G. Mainolfi, M. Petretta, and A. Cuocolo declare that they have no financial conflicts of interest.

References

1. Murthy VL, Naya M, Foster CR, Hainer J, Gaber M, Di Carli G, et al. Improved cardiac risk assessment with noninvasive measures of coronary flow reserve. *Circulation* 2011;124:2215-24.
2. Assante R, Zampella E, Arumugam P, Acampa W, Imbriaco M, Tout D, et al. Quantitative relationship between coronary artery calcium and myocardial blood flow by hybrid rubidium-82 PET/CT imaging in patients with suspected coronary artery disease. *J Nucl Cardiol* 2017;24:494-501.
3. Kajander SA, Joutsiniemi E, Saraste M, Pietilä M, Ukkonen H, Saraste A, et al. Clinical value of absolute quantification of myocardial perfusion with (15)O-water in coronary artery disease. *Circ Cardiovasc Imaging* 2011;4:678-84.
4. Zampella E, Acampa W, Assante R, Nappi C, Gaudieri V, Mainolfi CG, et al. Combined evaluation of regional coronary artery calcium and myocardial perfusion by (82)Rb PET/CT in the identification of obstructive coronary artery disease. *Eur J Nucl Med Mol Imaging* 2018;45:521-9.
5. Assante R, Acampa W, Zampella E, Arumugam P, Nappi C, Gaudieri V, et al. Prognostic value of atherosclerotic burden and coronary vascular function in patients with suspected coronary artery disease. *Eur J Nucl Med Mol Imaging* 2017;44:2290-8.
6. Ben-Haim S, Murthy VL, Breault C, Allie R, Sitek A, Roth N, Fantony J, et al. Quantification of myocardial perfusion reserve using dynamic SPECT imaging in humans: A feasibility study. *J Nucl Med* 2013;54:873-9.
7. de Souza ACDAH, Gonçalves BKD, Tedeschi AL, Lima RSL. Quantification of myocardial flow reserve using a gamma camera with solid-state cadmium-zinc-telluride detectors: Relation to angiographic coronary artery disease. *J Nucl Cardiol* 2019. <https://doi.org/10.1007/s12350-019-01775-z>.
8. Miyagawa M, Nishiyama Y, Uetani T, Ogimoto A, Ikeda S, Ishimura H, et al. Estimation of myocardial flow reserve utilizing an ultrafast cardiac SPECT: Comparison with coronary angiography, fractional flow reserve, and the SYNTAX score. *Int J Cardiol* 2017;244:347-53.
9. Ben Bouallègue F, Roubille F, Lattuca B, Cung TT, Macia JC, Gervasoni R, et al. SPECT Myocardial perfusion reserve in patients with multivessel coronary disease: Correlation with angiographic findings and invasive fractional flow reserve measurements. *J Nucl Med* 2015;56:1712-7.
10. Zavadovsky KV, Mochula AV, Boshchenko AA, Vrublevsky AV, Baev AE, Krylov AL, et al. Absolute myocardial blood flows derived by dynamic CZT scan vs invasive fractional flow reserve: Correlation and accuracy. *J Nucl Cardiol* 2019; <https://doi.org/10.1007/s12350-019-01678-z>.
11. Agostini D, Roule V, Nganoa C, Roth N, Baavour R, Parenti JJ, et al. First validation of myocardial flow reserve assessed by dynamic (99m)Tc-sestamibi CZT-SPECT camera: Head to head comparison with (15)O-water PET and fractional flow reserve in patients with suspected coronary artery disease. The WATERDAY study. *Eur J Nucl Med Mol Imaging* 2018;45:1079-90.
12. Nkoulou R, Fuchs TA, Pazhenkottal AP, Kuest SM, Ghadri JR, Stehli J, et al. Absolute myocardial blood flow and flow reserve assessed by gated SPECT with cadmium-zinc-telluride detectors using 99mTc-tetrofosmin: Head-to-head comparison with 13N-ammonia PET. *J Nucl Med* 2016;57:1887-92.
13. Driessen RS, Raijmakers PG, Stuijzand WJ, Knaapen P. Myocardial perfusion imaging with PET. *Int J Cardiovasc Imaging* 2017;33:1021-31.
14. Bateman TM, Dilsizian V, Beanlands RS, DePuey EG, Heller GV, Wolinsky DA. American Society of Nuclear Cardiology and Society of Nuclear Medicine and Molecular Imaging: Joint position statement on the clinical indications for myocardial perfusion PET. *J Nucl Med* 2016;57:1654-6.
15. Diamond GA, Forrester JS. Analysis of probability as an aid in the clinical diagnosis of coronary-artery disease. *N Engl J Med* 1979;300:1350-8.
16. Klein R, Renaud JM, Ziadi MC, Thorn SL, Adler A, Beanlands RS, deKemp RA. Intra- and inter-operator repeatability of myocardial blood flow and myocardial flow reserve measurements using rubidium-82 PET and a highly automated analysis program. *J Nucl Cardiol* 2010;17:600-16.
17. Nesterov SV, Deshayes E, Sciagrà R, Settimo L, Declerck JM, Pan XB, et al. Quantification of myocardial blood flow in absolute terms using (82)Rb PET imaging: The RUBY-10 Study. *JACC Cardiovasc Imaging* 2014;7:1119-27.
18. Fihn SD, Blankenship JC, Alexander KP, Ittl JA, Byrne JG, Fletcher BJ, et al. ACC/AHA/AATS/PCNA/SCAI/STS focused update of the guideline for the diagnosis and management of patients with stable ischemic heart disease: a report of the American College of Cardiology/American Heart Association Task Force on Practice Guidelines, and the American Association for Thoracic Surgery, Preventive Cardiovascular Nurses Association, Society for Cardiovascular Angiography and Interventions, and Society of Thoracic Surgeons. *J Am Coll Cardiol* 2014;2014(64):1929-49.
19. Petretta M, Acampa W, Daniele S, Petretta MP, Nappi C, Assante R, et al. Transient ischemic dilation in SPECT myocardial perfusion imaging for prediction of severe coronary artery disease in diabetic patients. *J Nucl Cardiol* 2013;20:45-52.
20. Bland JM, Altman D. Statistical methods for assessing agreement between two methods of clinical measurement. *Lancet* 1986;1:307-10.
21. Ruopp MD, Perkins NJ, Whitcomb BW, Schisterman EF. Youden index and optimal cut-point estimated from observations affected by a lower limit of detection. *Biomed J* 2008;50:419-30.
22. Mannarino T, Assante R, Ricciardi C, Zampella E, Nappi C, Gaudieri V, Mainolfi CG, Di Vaia E, Petretta M, Cesarelli M, Cuocolo A, Acampa W. Head-to-head comparison of diagnostic accuracy of stress-only myocardial perfusion imaging with conventional and cadmium-zinc telluride single-photon emission computed tomography in women with suspected coronary artery disease. *J Nucl Cardiol* 2019. <https://doi.org/10.1007/s12350-019-01789-7>.
23. Cuocolo A, Cittanti C, Acampa W, Larobina M, Petretta M. Current and future status of blood flow tracers. *Curr Cardiovasc Imaging Rep* 2011;4:227-36.
24. deKemp RA, Renaud JM, Klein R, Beanlands RS. Radionuclide tracers for myocardial perfusion imaging and blood flow quantification. *Cardiol Clin* 2016;34:37-46.
25. Wells RG, Marvin B, Poirier M, Renaud J, deKemp RA, Ruddy TD. Optimization of SPECT measurement of myocardial blood flow with corrections for attenuation, motion, and blood binding compared with PET. *J Nucl Med* 2017;58:2013-9.
26. Giubbini R, Bertoli M, Durmo R, Bonacina M, Peli A, Faggiano I, et al. Comparison between N(13)NH(3)-PET and (99m)Tc-Tetrofosmin-CZT SPECT in the evaluation of absolute myocardial blood flow and flow reserve. *J Nucl Cardiol* 2019. <https://doi.org/10.1007/s12350-019-01939-x>.

27. Acampa W, Assante R, Mannarino T, Zampella E, D'Antonio A, Buongiorno P, et al. Low-dose dynamic myocardial perfusion imaging by CZT-SPECT in the identification of obstructive coronary artery disease. *Eur J Nucl Med Mol Imaging* 2019. <https://doi.org/10.1007/s00259-019-04644-6>.
28. van Dijk JD, Jager PL, van Osch JAC, Khodaverdi M, van Dalen JA. Comparison of maximal Rubidium-82 activities for myocardial blood flow quantification between digital and conventional PET systems. *J Nucl Cardiol* 2019;26:1286-91.
29. Renaud JM, Yip K, Guimond J, Trottier M, Pibarot P, Turcotte E, et al. Characterization of 3-dimensional PET systems for accurate quantification of myocardial blood flow. *J Nucl Med* 2017;58:103-9.

Publisher's Note Springer Nature remains neutral with regard to jurisdictional claims in published maps and institutional affiliations.